

Detecting light stop pairs in coannihilation scenarios at the LHC

Zhao-Huan Yu¹, Xiao-Jun Bi¹, Qi-Shu Yan², and Peng-Fei Yin¹

¹*Laboratory of Particle Astrophysics, Institute of High Energy Physics,
Chinese Academy of Sciences, Beijing 100049, China and*

²*College of Physics Sciences, University of Chinese Academy of Sciences, Beijing 100049, China*

In this work, we study the light stop pair signals at the large hadron collider (LHC) in three coannihilation scenarios. In order to yield the desired dark matter (DM) relic density, the neutralino can coannihilate with stop, chargino and stau, respectively. Signatures of the first scenario can be probed at the LHC via the associated jet production processes $pp \rightarrow j + \tilde{t}\tilde{t}^*$ by tagging an energetic mono-jet and a large missing transverse energy. The signatures of the other two scenarios can be searched via the pair production process $pp \rightarrow \tilde{t}\tilde{t}^*$ by tagging energetic b-jets in the final states and a large missing transverse energy. We find that the LHC results at 7 TeV with 5 fb^{-1} of data can exclude the stop mass up to 220, 380 and 220 GeV for these three scenarios, respectively. While the 20 fb^{-1} dataset at 8 TeV is considered, the LHC can be expected to exclude the stop mass up to 340, 430 and 370 GeV.

PACS numbers: 12.60.Jv, 14.80.Ly

I. INTRODUCTION

It is well known that DM plays a crucial role in the large scale structure formation of the universe, however, its nature is still unclear. Solving the nature of DM particle is a key problem in the cosmology and particle physics. There are many theoretical DM candidates proposed in literature [1], among which the lightest supersymmetric particle (LSP) in the supersymmetry (SUSY) model with conserved R-parity is a very attractive and widely studied candidate [2]. Generally the lightest neutralino with mass around 100 GeV up to TeV is the LSP in many low scale SUSY models. It is possible to explore and test these models at the LHC.

The thermal relic density of neutralino which should be consistent with the WMAP measurement [3] sets a strong constraint on the SUSY parameter space. If the neutralino is wino or higgsino dominated, the interactions between neutralinos are strong enough to produce suitable DM relic density. However, if the neutralino is bino-like, some additional mechanisms are necessary to enhance the annihilation cross section and avoid the over-production of neutralino. For instance, the neutralinos can annihilate via a resonance with fairly large cross section, which is the favored case in the minimal supergravity model (mSUGRA) [4]. Except the resonance enhancement, coannihilation is another possible mechanism to enhance neutralino annihilation rate and produce the suitable DM relic density [5, 6]. Typically, efficient coannihilation requires the LSP neutralino and the next-to-lightest supersymmetric particle (NLSP) are nearly degenerate in mass. In mSUGRA there are some typical parameter regions with significant coannihilation effects. One is the low m_0 region where the stau can be quasi-degenerate with the neutralino in mass and coannihilates with the neutralino [7]. Another region is the so-called focus point region, where the neutralino is a bino-higgsino mixture. In this region the chargino can be light enough and induce a significant coannihilation effect [6].

It is interesting to notice that the colored superpartners, like gluino [8], stop [9] and sbottom [10], can also be the coannihilating partners of the LSP in the minimal supersymmetric standard model (MSSM). In such cases, the strong interactions between the NLSP particles can be more efficient to enhance the effective DM annihilation cross section and to reduce the DM relic density. Moreover, the degenerate LSP-NLSP spectra suggest the colored NLSP should also be light, and such particles might have large production cross sections at the hadron colliders, and can be within the reach of the LHC [11–15].

Recently, the LHC direct SUSY searches at $\sqrt{s} = 7, 8 \text{ TeV}$ with several fb^{-1} of data have set very strong bounds on the masses of gluino and the squark of the first two generations [16, 17]. However, if the colored NLSP is almost degenerate with the LSP, the final states of the colored NLSP decay from direct pair production are soft, and lead to a small reconstructed missing transverse energy (\cancel{E}_T). Such signals are hardly triggered and selected by the detectors. Therefore, considering the DM constraints, the LHC bounds on the colored SUSY partner masses may be relaxed. The light gluino, stop or sbottom can still be consistent with the recent LHC results [11–15].

To overcome the triggering problem, an additional energetic jet from initial state radiation is required. The new physics signals can be triggered by this energetic mono-jet and the large \cancel{E}_T [18, 19]. Although the cross section of this mono-jet process is smaller than that of direct NLSP pair production by a factor of ten or more if we require the transverse momentum of mono-jet is larger than 100 GeV, the well-reconstructed large \cancel{E}_T can efficiently suppress the standard model (SM) backgrounds, especially the QCD background. In literatures, such associated mono-jet production channel has been demonstrated to be workable in various coannihilation scenarios [13, 15].

In this work, we focus on the coannihilation scenarios with a light stop quark. It is well-known that the lighter stop \tilde{t}_1 can be the lightest colored supersymmetric particle due to the large top Yukawa coupling and large mass splitting terms in many SUSY models. The light stop is also well-motivated by the “naturalness” argument [20]. Meanwhile, the electroweak baryogenesis requires a light stop (say 100 GeV or so) to generate the first order phase transition [21]. In order to accommodate the data of the DM relic density, the stop-neutralino coannihilation scenarios have also been proposed in literatures. Recently, the LHC direct SUSY searches have set many constraints on the light stop-neutralino mass spectra, but the main results are only valid for the decay channel $\tilde{t}_1 \rightarrow t\tilde{\chi}_1^0$ [22, 23]. It is still necessary to explore how the LHC can constrain the coannihilation scenarios in the SUSY models.

In this work, we perform a more comprehensive study on the coannihilation scenarios with a light stop. We consider the following three scenarios: (1) \tilde{t}_1 - $\tilde{\chi}_1^0$ coannihilation scenario with $m_{\tilde{\chi}_1^0} \sim m_{\tilde{t}_1}$; (2) $\tilde{\chi}_1^\pm$ - $\tilde{\chi}_1^0$ coannihilation scenario with $m_{\tilde{\chi}_1^\pm} \sim m_{\tilde{\chi}_1^0} < m_{\tilde{t}_1}$; (3) $\tilde{\tau}_1$ - $\tilde{\chi}_1^0$ coannihilation scenario with $m_{\tilde{\chi}_1^0} \sim m_{\tilde{\tau}_1} < m_{\tilde{t}_1}$. For simplicity, the other supersymmetric particles are assumed to be much heavier here.

We use the associated mono-jet production channel to constrain the parameter space for the first scenario. For the later two scenarios [24–26], we consider the production channels $pp \rightarrow \tilde{t}_1\tilde{t}_1^* \rightarrow b\bar{b}\tilde{\chi}_1^+\tilde{\chi}_1^-$ and $pp \rightarrow \tilde{t}_1\tilde{t}_1^* \rightarrow b\bar{b}\nu_\tau\bar{\nu}_\tau\tilde{\tau}_1^+\tilde{\tau}_1^-$. The cross sections of the electroweak supersymmetric particle direct productions, such as $pp \rightarrow \chi^0\chi^\pm$ and $pp \rightarrow \tilde{\tau}\tilde{\tau}^*$, are much smaller than those of the strong interaction. Therefore stop pair production $pp \rightarrow t\bar{t}^*$ can provide an advantage to probe these two scenarios. Since the chargino/stau is nearly degenerate with the LSP and the soft jets/taus from chargino/stau decay can hardly be successfully reconstructed, we find that the latest results from b-jets + \cancel{E}_T searches can put constraints on the parameter space. We would like to point out that the constraints from the LHC on the stop signatures in these two scenarios are new and have not been widely studied in literatures.

This paper is organized as follows. In Section II, for the \tilde{t}_1 - $\tilde{\chi}_1^0$ coannihilation scenario, we investigate the associated mono-jet production at the LHC and explore the constraints on the parameter space by the latest monojet + \cancel{E}_T searches. We also explore the parameter region feasible with the 20 fb^{-1} dataset at the collision energy $\sqrt{s} = 8\text{ TeV}$. In Section III, we focus on two coannihilation scenarios with a light stop quark where $\tilde{\chi}_1^\pm$ - $\tilde{\chi}_1^0$ and $\tilde{\tau}_1$ - $\tilde{\chi}_1^0$ are almost degenerate, respectively. We find that the searching channel of b-jets + \cancel{E}_T can put constraints on the allowed parameter space. We end this work in Section IV with discussions and conclusions.

II. STOP-NEUTRALINO COANNIHILATION SCENARIO

In this section we study the stop pair signature in the \tilde{t}_1 - $\tilde{\chi}_1^0$ coannihilation scenario. The NLSP is assumed to be the lighter stop \tilde{t}_1 . Coannihilation with the LSP $\tilde{\chi}_1^0$ requires that \tilde{t}_1 is slightly heavier than $\tilde{\chi}_1^0$, saying $(m_{\tilde{t}_1} - m_{\tilde{\chi}_1^0})/m_{\tilde{\chi}_1^0} \lesssim 20\%$ [27]. Then the decay modes $\tilde{t}_1 \rightarrow t\tilde{\chi}_1^0$ and $\tilde{t}_1 \rightarrow bW\tilde{\chi}_1^0$ would be kinematically forbidden. The loop-induced flavor changing neutral current decay mode $\tilde{t}_1 \rightarrow c\tilde{\chi}_1^0$ becomes dominant, since the four-body decay modes $\tilde{t}_1 \rightarrow ff'b\tilde{\chi}_1^0$ are strongly suppressed by the small phase space. Thus for the parameter region of $m_{\tilde{\chi}_1^0} + m_c \leq m_{\tilde{t}_1} < m_{\tilde{\chi}_1^0} + m_b + m_W$, we simply assume the branching ratio of $\tilde{t}_1 \rightarrow c\tilde{\chi}_1^0$ is 100%. Since the jets from stop decays are very soft and hardly reconstructed, we consider the production channel of a stop pair $\tilde{t}_1\tilde{t}_1^*$ associated with at least one hard QCD jet.

Using the final states of monojet + \cancel{E}_T to search for new physics, such as large extra dimension and effective DM interaction operators, have been performed by ATLAS [33] and CMS [34] collaborations at $\sqrt{s} = 7\text{ TeV}$ with the integrated luminosities of 4.7 fb^{-1} and 5.0 fb^{-1} , respectively. The crucial kinematic cuts used in these analyses are summarized in Table I. Events in the monojet + \cancel{E}_T channel are those contained large \cancel{E}_T and an energetic leading jet. Events with isolated leptons or more than two jets with $p_T > 30\text{ GeV}$ are rejected. The cuts $\Delta\phi(\vec{j}_2, \vec{\cancel{E}}_T) > 0.5$ and $\Delta\phi(\vec{j}_1, \vec{j}_2) < 2.5$ are used to suppress QCD multi-jet background events, where the large \cancel{E}_T may come from inefficient measurements of jets. Table I also tabulates the corresponding observed 95% CL upper limits on the beyond standard model (BSM) visible cross section $\sigma_{\text{vis}}^{\text{BSM}} \equiv \sigma \cdot A \cdot \epsilon$, which is defined as the production cross section times acceptance and efficiency. In the following study, we apply these latest limits to put bounds on the parameter space of the \tilde{t}_1 - $\tilde{\chi}_1^0$ coannihilation scenario.

In our simulation, the parton-level events of SUSY processes $pp \rightarrow \tilde{t}_1\tilde{t}_1^*$, $pp \rightarrow \tilde{t}_1\tilde{t}_1^* + \text{jets}$ and SM backgrounds are generated by MadGraph5 [28]. PYTHIA6 [29] is used to perform parton shower, particle decay and hadronization processes. Fast detector simulation is carried out by PGS4 [30]. The MLM matching scheme with p_T -ordered showers implemented in MadGraph5 is adopted to overcome the parton-jet double counting issue. For the stop production processes, the Q_{cut} parameter is chosen as 80 GeV which can yield the smooth jet distributions. Jets are reconstructed by using the anti- k_T clustering algorithm with a distance parameter $R = 0.4/0.5$ for ATLAS/CMS searches. The cross section of the stop pair production including the NLO corrections is calculated by Prospino2 [31]. For the top pair production, the K -factor is calculated by MCFM [32].

The dominant SM backgrounds for this searching channel are $Z(\rightarrow \nu\bar{\nu}) + \text{jets}$ and $W(\rightarrow \ell\nu) + \text{jets}$. For the $W(\rightarrow \ell\nu) + \text{jets}$ process, charged leptons may be clustered into a jet or missed along the beam pile lines. The

	ATLAS 7 TeV, 4.7 fb ⁻¹	CMS 7 TeV, 5.0 fb ⁻¹	LHC 8 TeV, 20 fb ⁻¹
Signal region	SR1/SR2/SR3/SR4		
\cancel{E}_T [GeV] >	120/220/350/500	250/300/350/400	300
$p_T^{j_1}$ [GeV] >	120/220/350/500 ($ \eta < 2$)	110 ($ \eta < 2.4$)	150 ($ \eta < 2.4$)
$p_T^{j_2}$ [GeV] <	30	30	50
	$\Delta\phi(\vec{j}_2, \vec{\cancel{E}}_T) > 0.5$	$\Delta\phi(\vec{j}_1, \vec{j}_2) < 2.5$	
	Lepton veto		
$\sigma_{\text{vis}}^{\text{BSM}}$ [fb] <	1920/170/30/6.9 (95% CL)	120/73.6/31.6/19 (95% CL)	22.7/37.9 ($S/\sqrt{B} < 3/5$)

TABLE I: Crucial kinematic cuts in the ATLAS [33] and CMS [34] monojet + \cancel{E}_T analyses as well as that in our monojet + \cancel{E}_T analysis for 20 fb⁻¹ at the LHC with $\sqrt{s} = 8$ TeV are tabulated. The observed 95% CL upper limits on the BSM visible cross section $\sigma_{\text{vis}}^{\text{BSM}}$ in the ATLAS and CMS analyses are provided, as well as the expected upper limits on $\sigma_{\text{vis}}^{\text{BSM}}$ for $S/\sqrt{B} = 3$ and 5 in our analysis at 8 TeV.

irreducible background $Z(\rightarrow \nu\bar{\nu}) + \text{jets}$ is most important. To validate our MC results, we match the number of events of the SM background in our simulation to those provided by the ATLAS and CMS collaborations. We find that the corresponding rescaling factors of our simulation are 1.05, 0.97, 0.92 and 0.86 for the signal regions SR1, SR2, SR3 and SR4 in the ATLAS analysis, while they are 0.98, 0.91, 0.96 and 0.97 for the signal regions with $\cancel{E}_T > 250, 300, 350$ and 400 GeV in the CMS analysis. These rescaling factors are then applied to normalize the signal events of $\tilde{t}_1\tilde{t}_1^* + \text{jets}$ in our simulation.

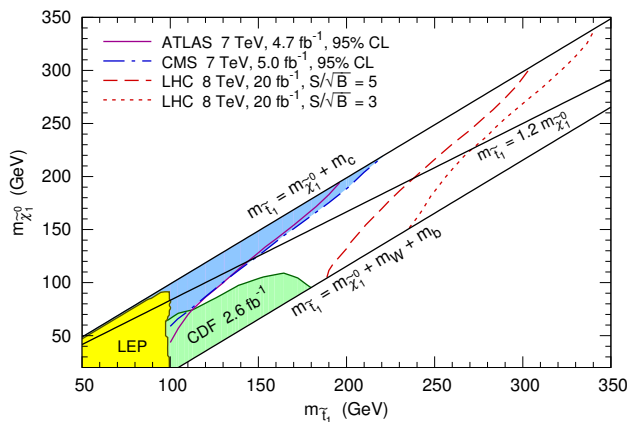


FIG. 1: The 95% CL exclusion limits by ATLAS and CMS monojet + \cancel{E}_T analyses at 7 TeV and signal significances predicted at 8 TeV in the $m_{\tilde{t}_1} - m_{\tilde{\chi}_1^0}$ parameter plane of the $\tilde{t}_1 - \tilde{\chi}_1^0$ coannihilation scenario are provided. In contrast, the yellow and green regions show the excluded regions by LEP and CDF, respectively.

The observed 95% CL exclusion limits on mass parameter space in the $\tilde{t}_1 - \tilde{\chi}_1^0$ coannihilation scenario are presented in Fig. 1. We show the regions excluded by the ATLAS and CMS analyses. In contrast, we also show the yellow and green regions, which have been excluded by LEP and CDF [35], respectively. Obviously, the LHC has demonstrated its unique potential to probe the $\tilde{t}_1 - \tilde{\chi}_1^0$ coannihilation scenario.

As the mass splitting $m_{\tilde{t}_1} - m_{\tilde{\chi}_1^0}$ becomes smaller, the charm quarks from \tilde{t}_1 decays become less energetic, and so do their resulting jets. The only energetic jet must be produced from initial state radiation and is opposite to the stop pair direction. Thus the large \cancel{E}_T can be successfully reconstructed and used to trigger the signals. Obviously, for a fixed value of $m_{\tilde{t}_1}$, a smaller $m_{\tilde{t}_1} - m_{\tilde{\chi}_1^0}$ means more easily being detected by the monojet + \cancel{E}_T analysis, as demonstrated in Fig. 1.

The region between the two lines labelled by “ $m_{\tilde{t}_1} = m_{\tilde{\chi}_1^0} + m_c$ ” and by “ $m_{\tilde{t}_1} = 1.2m_{\tilde{\chi}_1^0}$ ” is considered as the so-called “coannihilation region” and is excluded up to $m_{\tilde{t}_1} \simeq 150 - 220$ GeV by the LHC collaborations. The most stringent limit is put by CMS and can reach up to $m_{\tilde{t}_1} \simeq 220$ GeV. The results of ATLAS agree with those obtained by the CMS. Obviously, with more dataset, like the dataset of 20 fb⁻¹ at $\sqrt{s} = 8$ TeV, more parameter region can be excluded, as shown in Fig. 1.

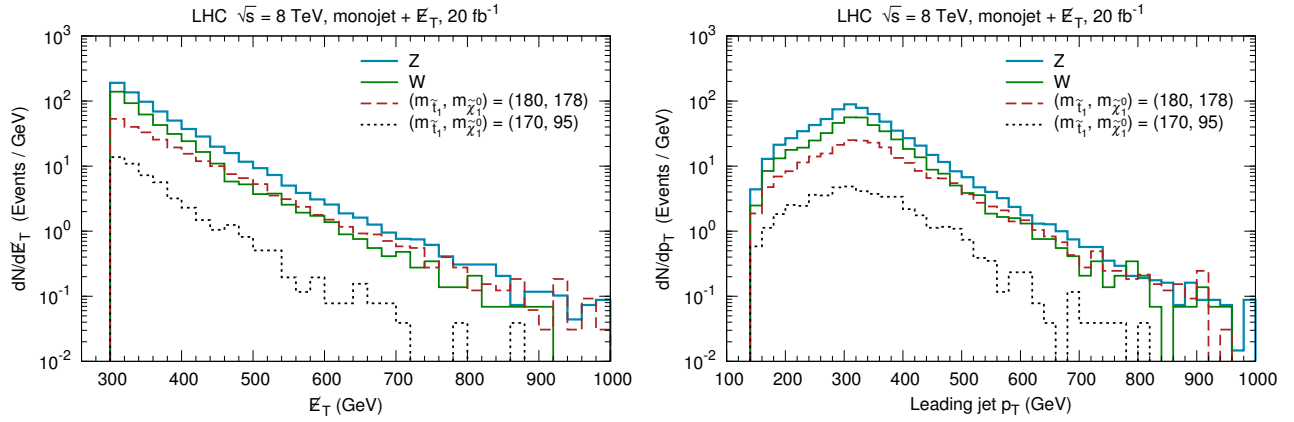


FIG. 2: The \cancel{E}_T and the leading jet p_T distributions for the SM backgrounds and two benchmark signal points in the $\tilde{t}_1\text{-}\tilde{\chi}_1^0$ coannihilation scenario at the LHC with $\sqrt{s} = 8$ TeV for 20 fb^{-1} are shown.

Now we look closely at our results for the LHC with a dataset of 20 fb^{-1} at $\sqrt{s} = 8$ TeV. After applying the cuts listed in the last column of Table I, we arrive at a total number of SM background events $B = 22944$ which includes $13939 Z(\rightarrow \nu\bar{\nu}) + \text{jets}$ and $9005 W(\rightarrow \ell\nu) + \text{jets}$ events. With this number, we can have the visible cross section of BSM $\sigma_{\text{vis}}^{\text{BSM}} = 22.7\text{ fb}$ (37.9 fb) corresponding to the significance $S/\sqrt{B} = 3$ (5).

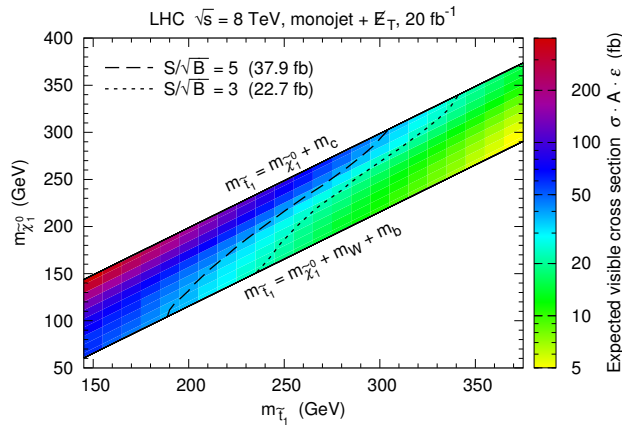


FIG. 3: Expected BSM visible cross section in the $\tilde{t}_1\text{-}\tilde{\chi}_1^0$ coannihilation scenario at the LHC with $\sqrt{s} = 8$ TeV for 20 fb^{-1} is shown. The short (long) dash line corresponds to $S/\sqrt{B} = 3$ (5).

We also present the distributions of \cancel{E}_T and the leading jet p_T in Fig. 2, where the line shapes of two main SM backgrounds and two benchmark points of SUSY model are shown. In these two benchmark points, $(m_{\tilde{t}_1}, m_{\tilde{\chi}_1^0})$ are deliberately chosen as $(180, 178)$ and $(170, 95)$ GeV to represent a nearly-degenerate and a moderate splitting mass spectra, respectively. It is noticed that all the lines in the leading jet p_T distribution peak at ~ 300 GeV, which can be attributed to the fact that in most events the \cancel{E}_T approaches the cut threshold 300 GeV and $\vec{\cancel{E}}_T$ is mainly balanced by the leading jet in the transverse plane. We also find that the kinetic variable distributions of the “nearly-degenerate” benchmark point fall off more slowly than those of the SM backgrounds. Nonetheless, increasing the cut conditions of \cancel{E}_T and the leading jet p_T can cause a sizable loss of signal with moderately suppressing the backgrounds. In order to reduce the irreducible backgrounds, we have to go beyond these kinematic cuts.

In Fig. 3, we show the expected BSM visible cross section in the $m_{\tilde{t}_1}\text{-}m_{\tilde{\chi}_1^0}$ plane. The short (long) dash line corresponds to $S/\sqrt{B} = 3$ (5) and is also plotted in Fig. 1 for comparison. In the “coannihilation region”, the region with $S/\sqrt{B} > 3$ (5) reaches $m_{\tilde{t}_1} \simeq 270 - 340$ GeV ($240 - 300$ GeV).

III. CHARGINO/STAU-NEUTRALINO COANNIHILATION SCENARIO

In this section, we study the stop pair signature $pp \rightarrow \tilde{t}\tilde{t}^*$ in two coannihilation scenarios where $\tilde{\chi}_1^0$ coannihilates with $\tilde{\chi}_1^\pm$ and $\tilde{\tau}_1$, respectively. Here we would like to point out that if these particles are mainly produced by stop decays the LHC SUSY searches with tagged b-jets are suitable to test such scenarios.

In the $\tilde{\chi}_1^\pm - \tilde{\chi}_1^0$ coannihilation scenario, the NLSP chargino $\tilde{\chi}_1^\pm$ is nearly degenerate with $\tilde{\chi}_1^0$ in mass, saying $(m_{\tilde{\chi}_1^\pm} - m_{\tilde{\chi}_1^0})/m_{\tilde{\chi}_1^0} \lesssim 20\%$ [27]. We focus on the situation where the produced stop \tilde{t}_1 decays into $b\tilde{\chi}_1^+$. Because two-body decay channels of $\tilde{\chi}_1^+$, such as $\tilde{\chi}_1^+ \rightarrow W^+\tilde{\chi}_1^0$ and $\tilde{\chi}_1^+ \rightarrow \nu\tilde{\tau}_1$, would be kinematically closed, $\tilde{\chi}_1^+$ dominantly decays into $\tilde{\chi}_1^0$ and soft leptons or quarks. In this case, the exact value of $m_{\tilde{\chi}_1^\pm} - m_{\tilde{\chi}_1^0}$ is of less importance because the soft products from $\tilde{\chi}_1^+$ decay can hardly be reconstructed by detectors. Therefore, we fix $(m_{\tilde{\chi}_1^\pm} - m_{\tilde{\chi}_1^0})/m_{\tilde{\chi}_1^0}$ to be 10% as a typical case in the coannihilation scenario. Furthermore, we assume the branching ratio of $\tilde{t}_1 \rightarrow b\tilde{\chi}_1^+$ is 100% in the region of $m_b + m_{\tilde{\chi}_1^\pm} \leq m_{\tilde{t}_1} \leq m_{\tilde{\chi}_1^0} + m_t$.

Although the decay products from $\tilde{\chi}_1^+$ are soft, the b quarks from stop decays can be energetic enough to be tagged. Meanwhile, the b-tagging technology is found to be powerful to suppress the SM backgrounds. Therefore the final state with b-jets + \cancel{E}_T can be used to constrain this scenario. The main SM background events are from production processes of top pair, single top, $Z(\rightarrow \nu\bar{\nu})$ + heavy flavors and $W(\rightarrow \ell\nu)$ + heavy flavors.

	ATLAS 7 TeV, 2.05 fb ⁻¹	ATLAS 7 TeV, 4.7 fb ⁻¹	
Signal region		SR2	SR3a
\cancel{E}_T [GeV] >	130	200	150
Leading jet	$p_T > 130$ GeV, b-tagged	$p_T > 60$ GeV, b-tagged	$p_T > 130$ GeV
2nd leading jet	$p_T > 50$ GeV, b-tagged	$p_T > 60$ GeV, b-tagged	$p_T > 30$ GeV, b-tagged
3rd leading jet	$p_T < 50$ GeV	$p_T < 50$ GeV	$p_T > 30$ GeV, b-tagged
	$m_{CT} > 100$ GeV		$\Delta\phi(\vec{j}_1, \vec{\cancel{E}}_T) > 2.5$
	$\Delta\phi(\vec{j}_{1,2}, \vec{\cancel{E}}_T) > 0.4$		$\Delta\phi(\vec{j}_{2,3}, \vec{\cancel{E}}_T) > 0.4$
	$\cancel{E}_T/m_{\text{eff}} > 0.25$, lepton veto		
$\sigma_{\text{vis}}^{\text{BSM}}$ [fb] <	13.4 (95% CL)	2.29 (95% CL)	7.83 (95% CL)

TABLE II: Kinematic cuts in the ATLAS 2 b-jets + \cancel{E}_T analysis for 2.05 fb⁻¹ [36] and in the updated analysis for 4.7 fb⁻¹ [37] at the LHC with $\sqrt{s} = 7$ TeV are tabulated. The observed 95% CL upper limits on $\sigma_{\text{vis}}^{\text{BSM}}$ are also given.

	CMS 7 TeV, 4.98 fb ⁻¹	LHC 8 TeV, 20 fb ⁻¹
Signal region	1BL	$\geq 1\text{BL}$
\cancel{E}_T [GeV] >	250	200
	$N_{\text{jet}}(p_T > 50 \text{ GeV}) \geq 3$	$N_{\text{jet}}(p_T > 60 \text{ GeV}) \geq 3$
H_T [GeV] >	400	300
	$\Delta\hat{\phi}_{\text{min}} > 4.0$	$\Delta\phi(\vec{j}_{1,2,3}, \vec{\cancel{E}}_T) > 0.4$
	At least one jet with $p_T > 30$ GeV tagged as b-jet	
	Lepton veto	
	-	$m_{jjj} \notin (130, 200)$ GeV
$\sigma_{\text{vis}}^{\text{BSM}}$ [fb] <	20.6 (95% CL)	8.4/14.0 ($S/\sqrt{B} < 3/5$)

TABLE III: Kinematic cuts in the CMS b-jets + \cancel{E}_T analysis [38] at $\sqrt{s} = 7$ TeV, and in our analysis for ≥ 1 b-jets + \cancel{E}_T final state for 20 fb⁻¹ at the LHC with $\sqrt{s} = 8$ TeV are tabulated. The observed 95% CL upper limit $\sigma_{\text{vis}}^{\text{BSM}}$ in the CMS analysis is given, so are the expected upper limits on $\sigma_{\text{vis}}^{\text{BSM}}$ for $S/\sqrt{B} = 3$ and 5 in our analysis at 8 TeV.

The ATLAS collaboration has reported the BSM searching in the 2 b-jets + \cancel{E}_T channel at $\sqrt{s} = 7$ TeV with 2.05 fb⁻¹ [36] and 4.7 fb⁻¹ [37] of data. On the other hand, the CMS collaboration has also released results in the b-jets + \cancel{E}_T channel at $\sqrt{s} = 7$ TeV with 4.98 fb⁻¹ [38] of data. The kinematic cuts used in these analyses are summarized in Table II and III, where the crucial cuts in the signal regions are tabulated. The observed 95% CL upper limits on $\sigma_{\text{vis}}^{\text{BSM}}$ are also given in the tables.

Following the method proposed in Ref. [19], we estimate the observed 95% CL upper limit on the number of BSM events N_{BSM} by requiring

$$\chi^2 \equiv \frac{(N_{\text{obs}} - N_{\text{SM}} - N_{\text{BSM}})^2}{N_{\text{SM}} + \sigma_{\text{SM}}^2 + N_{\text{BSM}}} = 3.841, \quad (1)$$

where N_{obs} is the number of observed events, N_{SM} is the number of estimated SM background events, and σ_{SM} is the uncertainty of N_{SM} including statistic and systematic uncertainties. The 95% CL upper limit on $\sigma_{\text{vis}}^{\text{BSM}}$ is obtained by dividing N_{BSM} by integrated luminosity. For instances, the expected BSM visible cross sections in the signal region SR2 of the ATLAS search and in the signal region 1BL of the CMS search are shown in Fig. 4, where the solid lines correspond to the observed 95% CL exclusion limits. The 95% CL exclusion limits corresponding to several signal regions in ATLAS and CMS searches at 7 TeV in the $m_{\tilde{t}_1} - m_{\tilde{\chi}_1^\pm}$ plane are also derived, as shown in Fig. 5.

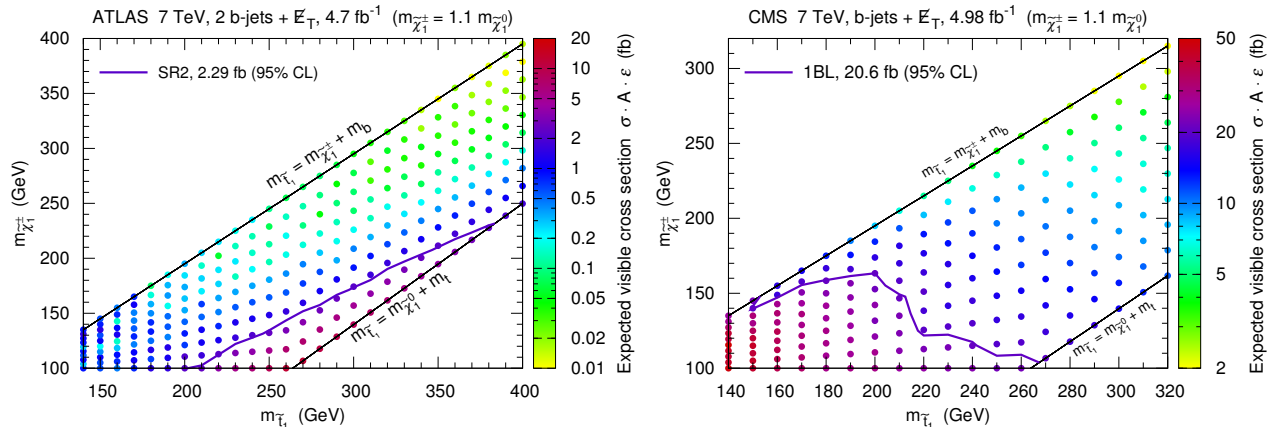


FIG. 4: Expected BSM visible cross sections for the signal region SR2 of the ATLAS search (left frame) and for the signal region 1BL of the CMS search (right frame) in the $\tilde{\chi}_1^\pm - \tilde{\chi}_1^0$ coannihilation scenario at $\sqrt{s} = 7$ TeV are shown. The solid lines correspond to the observed 95% CL exclusion limits.

Below we discuss the ATLAS analysis approaches in more details. In the first and second approaches, the ATLAS searches focus on the events with two b-jets and consider two types of kinematic variables. 1) It requires that there must be exactly two hard jets ($p_T > 50 - 60$ GeV) and both of them are b-tagged. To satisfy this requirement, the mass splitting between \tilde{t}_1 and $\tilde{\chi}_1^\pm$ should be large enough. 2) In addition the contranverse mass $m_{\text{CT}} = \sqrt{(E_T^{j_1} + E_T^{j_2})^2 - (\mathbf{p}_T^{j_1} - \mathbf{p}_T^{j_2})^2}$ is required to be larger than 100 GeV. For stop pair events in the $\tilde{\chi}_1^\pm - \tilde{\chi}_1^0$ coannihilation scenario, the distribution of m_{CT} has an endpoint at $m_{\text{CT}}^{\text{max}} = (m_{\tilde{t}_1}^2 - m_{\tilde{\chi}_1^\pm}^2)/m_{\tilde{t}_1}$, which can be achieved when the two b-jets are co-linear. Thus when the masses of \tilde{t}_1 and $\tilde{\chi}_1^\pm$ are close, stop pair events can hardly satisfy the condition $m_{\text{CT}} > 100$ GeV. On the other hand, this condition also rejects quite many top pair events of which the values of m_{CT} are often smaller than 100 GeV.

It is found that these two types of cut conditions enable the first two analysis approaches much easier to select out SUSY events with $m_{\tilde{t}_1} - m_{\tilde{\chi}_1^\pm} \gtrsim 100$ GeV, which can be read out in the left frame of Fig. 4. For $m_{\tilde{t}_1} = m_{\tilde{\chi}_1^0} + m_t$, using the ATLAS searching result of the signal region SR2, the 95% CL exclusion limit can reach up to $m_{\tilde{t}_1} \simeq 380$ GeV.

In the third analysis approach, it requires a hard leading jet which is not a b-jet, and the two b-jets can be soft. For stop pair events, this approach tends to select the events with an high p_T jet from initial state radiation which recoils against the stop pair system. Then this jet and the missing transverse momentum are almost back-to-back, and the condition $\Delta\phi(\vec{j}_1, \vec{\cancel{E}}_T) > 2.5$ is useful to reduce SM backgrounds without losing many signal events. As a result, the number of selected SUSY events mainly depends on the production cross section and is not so sensitive to $m_{\tilde{t}_1} - m_{\tilde{\chi}_1^\pm}$. Therefore in Fig. 5, the ATLAS searching result of the signal region SR3a excludes a large region for $m_{\tilde{t}_1} \lesssim 240$ GeV.

The signal region 1BL in the CMS search focuses on events with at least one b-jet. It is required that there are at least three hard jets with $p_T > 50$ GeV, and the scalar sum of their p_T , H_T , is demanded to be larger than 400 GeV. Events of stop pair production associating with initial state radiation jets are easier to be selected. The selection condition on b-jet is so loose that just more than one b-jet with $p_T > 30$ GeV is required. Consequently, for $m_{\tilde{t}_1} \lesssim 200$ GeV, even the region where $m_{\tilde{\chi}_1^\pm}$ closes to $m_{\tilde{t}_1}$ can be excluded, as shown in Figs. 4 and 5.

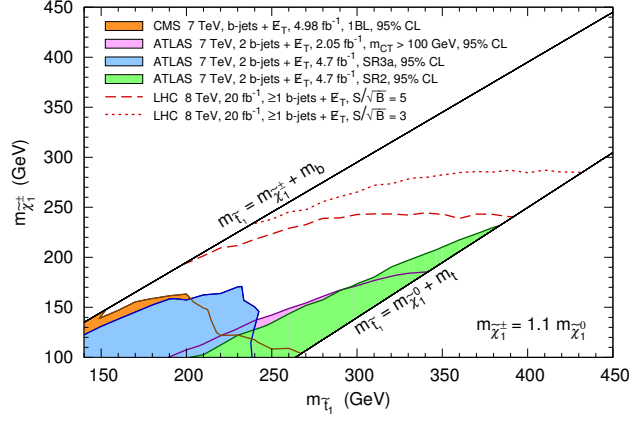


FIG. 5: 95% CL exclusion limits corresponding to several signal regions in ATLAS and CMS searches at 7 TeV and signal significances predicted at 8 TeV in the $m_{\tilde{\tau}_1}$ - $m_{\tilde{\chi}_1^\pm}$ plane of the $\tilde{\chi}_1^\pm$ - $\tilde{\chi}_1^0$ coannihilation scenario.

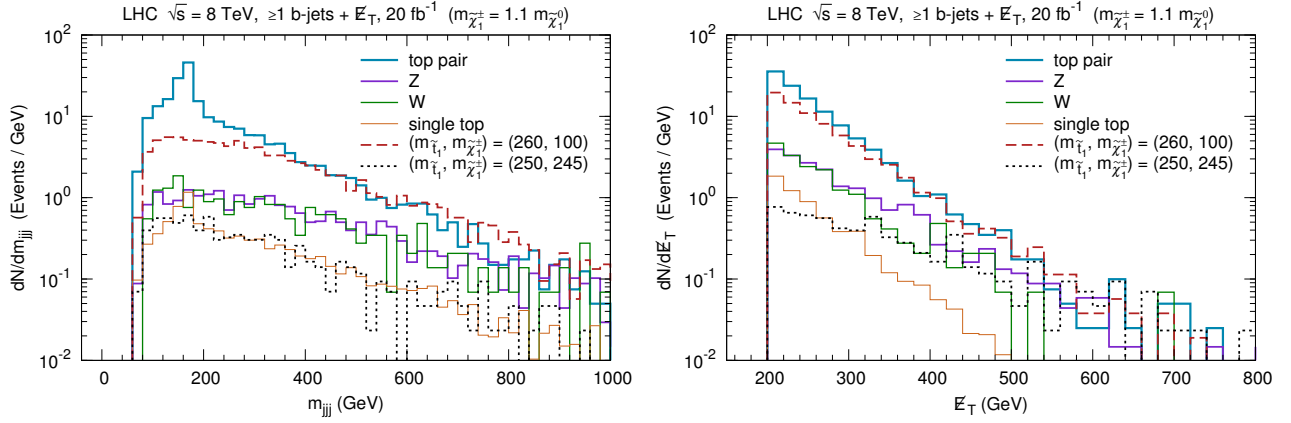


FIG. 6: The m_{jjj} and E_T distributions for the SM backgrounds and two benchmark points in the $\tilde{\chi}_1^\pm$ - $\tilde{\chi}_1^0$ coannihilation scenario at the LHC with $\sqrt{s} = 8$ TeV for 20 fb^{-1} are shown. The m_{jjj} distributions are plotted before applying the condition $m_{jjj} \notin (130, 200)$ GeV.

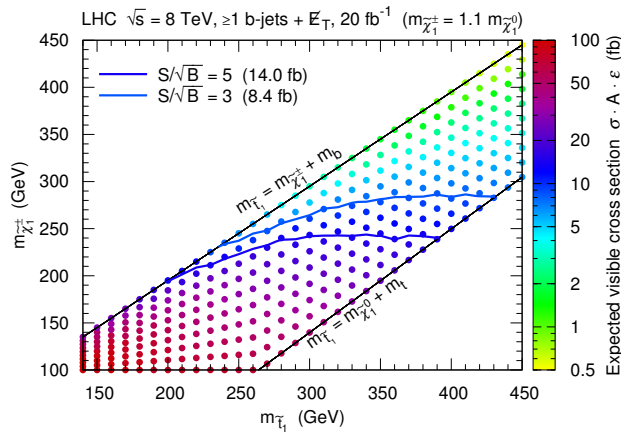


FIG. 7: Expected BSM visible cross section in the $\tilde{\chi}_1^\pm$ - $\tilde{\chi}_1^0$ coannihilation scenario at the LHC with $\sqrt{s} = 8$ TeV for 20 fb^{-1} are presented. The solid lines correspond to $S/\sqrt{B} = 3$ and 5 , respectively.

At the LHC with $\sqrt{s} = 8$ TeV and the luminosity of 20 fb^{-1} , we adopted the analysis approach listed in the second column of Table III. It is similar to the cut used in the signal region 1BL of the CMS search. However, we choose lower cut conditions of \cancel{E}_T and H_T in order to select more signal events.

Furthermore, in order to suppress the $t\bar{t}$ background, we consider a variable m_{jjj} . It has been used in the ATLAS search [23], where it is applied to pick out hadronically decaying tops instead of rejecting them. To construct m_{jjj} , a pair of jets with invariant mass $m_{jj} > 60$ GeV and smallest ΔR is picked out and reconstructed as a hadronically decaying W boson. A third jet which is closest to the reconstructed W boson is also selected. Then m_{jjj} is the invariant mass of these three jets, which may be the decay products of a hadronically decaying top. In the events of top pair and single top production processes, the distributions of m_{jjj} nearly peak at the mass of top quark $m_t = 173$ GeV. This feature looks so clear in the left frame of Fig. 6, where all the selection conditions in the kinematic cut are applied except for the condition on m_{jjj} . Then we can see that rejecting events with $m_{jjj} \in (130, 200)$ GeV is useful to suppress top pair and single top backgrounds. It can reject 47% (31%) of top pair (single top) events, while only rejects 20% (21%) of stop events for $m_{\tilde{t}_1} = 260$ (250) GeV and $m_{\tilde{\chi}_1^\pm} = 100$ (245) GeV. In the right frame of Fig. 6, the \cancel{E}_T distributions are also shown.

After applying all cuts, we arrive at a total number of SM background events $B = 3132$ which includes 2269 top pair events, 390 $Z(\rightarrow \nu\bar{\nu}) + \text{hf}$ events, 353 $W(\rightarrow \ell\nu) + \text{hf}$ events and 120 single top events. Consequently, $S/\sqrt{B} = 3$ (5) corresponds to BSM visible cross section $\sigma_{\text{vis}}^{\text{BSM}} = 8.4$ fb (14.0 fb). Fig. 7 shows the expected $\sigma_{\text{vis}}^{\text{BSM}}$ in the $m_{\tilde{t}_1} - m_{\tilde{\chi}_1^\pm}$ plane of the $\tilde{\chi}_1^\pm - \tilde{\chi}_1^0$ coannihilation scenario. The limits correspond to $S/\sqrt{B} = 3$ and 5 are plotted in both Figs. 5 and 7.

These limits are nearly horizontal in the $m_{\tilde{t}_1} - m_{\tilde{\chi}_1^\pm}$ plane due to the following reason. In general, when $m_{\tilde{t}_1}$ is fixed, stop events with larger $m_{\tilde{t}_1} - m_{\tilde{\chi}_1^\pm}$ are easier to induce hard jets and pass the kinematic cut. When $m_{\tilde{t}_1} - m_{\tilde{\chi}_1^\pm}$ is small, it needs small $m_{\tilde{t}_1}$, which corresponds to large production cross section, to yield more events to reach higher signal significance. The region with $S/\sqrt{B} > 3$ (5) almost covers all the space with $m_{\tilde{\chi}_1^\pm} \lesssim 280$ (240) GeV and reaches $m_{\tilde{t}_1} \simeq 430$ (390) GeV.

Finally, we study the $\tilde{\tau}_1 - \tilde{\chi}_1^0$ coannihilation scenario. In many SUSY scenario stau can be light and less constrained by direct search at the LHC. If stau is produced by decays of charginos and heavier neutralinos, the isolated tau in the final states is helpful to suppress the SM background. Especially, if the final states of SUSY events contain tau and other charged leptons or b-jets, the signatures can be well-reconstructed. However, in the stau-neutralino coannihilation scenario, the NLSP $\tilde{\tau}_1$ and the LSP $\tilde{\chi}_1^0$ are nearly degenerate in mass, the τ leptons from the stau decay $\tilde{\tau}_1 \rightarrow \tau\tilde{\chi}_1^0$ would be soft and can hardly be identified by detectors. In this work, we fix the relation $m_{\tilde{\tau}_1} = 1.1m_{\tilde{\chi}_1^0}$. We focus on the stop decay channel $\tilde{t}_1 \rightarrow b\tilde{\tau}_1^+ \nu_\tau$ and assume that its branching ratio is 100% for $m_b + m_{\tilde{\tau}_1} \leq m_{\tilde{t}_1} \leq m_{\tilde{\chi}_1^0} + m_t$.

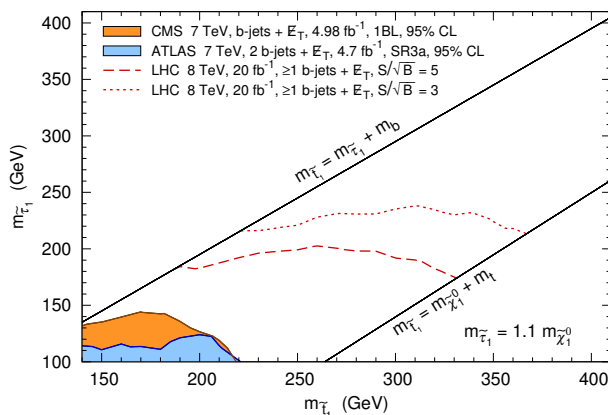


FIG. 8: The 95% CL exclusion limits corresponding to signal regions in ATLAS and CMS searches at 7 TeV and signal significances predicted at 8 TeV in the $m_{\tilde{t}_1} - m_{\tilde{\tau}_1}$ plane of the $\tilde{\tau}_1 - \tilde{\chi}_1^0$ coannihilation scenario are provided.

The situation seems similar to that in the $\tilde{\chi}_1^\pm - \tilde{\chi}_1^0$ coannihilation scenario. Due to the 3-body decay, however, the b quark from stop decay tends to be softer and it is not easy to be tagged. In addition, there are four sources of missing transverse momentum, two neutrinos and two neutralinos. The \cancel{E}_T might be small when the momenta of these four particles cancel out among themselves. Because of these reasons, provided the same kinematic cuts, exclusion limits by ATLAS and CMS searches at 7 TeV and signal significance predicted at 8 TeV are all much weaker than those in

the $\tilde{\chi}_1^\pm - \tilde{\chi}_1^0$ coannihilation scenario, as demonstrated in Fig. 8. In the $m_{\tilde{t}_1} - m_{\tilde{\tau}_1}$ plane, the ATLAS and CMS searches just exclude a small region up to $m_{\tilde{t}_1} \simeq 220$ GeV. At the LHC with $\sqrt{s} = 8$ TeV for 20 fb^{-1} , using the same kinematic cut we adopted before, the region with $S/\sqrt{B} > 3$ (5) reaches $m_{\tilde{\tau}_1} \simeq 240$ (200) GeV and $m_{\tilde{t}_1} \simeq 370$ (330) GeV.

IV. CONCLUSIONS AND DISCUSSIONS

In this work, we investigate the impacts of coannihilation scenarios on the light stop searches at the LHC. For the $\tilde{t}_1 - \tilde{\chi}_1^0$ coannihilation scenario, the best searching channel is monojet + \cancel{E}_T . Using the latest LHC mono-jet results, the present excluded region is up to $m_{\tilde{t}_1} \simeq 150 - 220$ GeV for the coannihilation condition $(m_{\tilde{t}_1} - m_{\tilde{\chi}_1^0})/m_{\tilde{\chi}_1^0} \lesssim 20\%$. Comparing with previous studies [13], the present mass bound has been improved to higher value. At the LHC with $\sqrt{s} = 8$ TeV for 20 fb^{-1} , the region with $S/\sqrt{B} > 3$ is expected to reach up to $m_{\tilde{t}_1} \simeq 340$ GeV.

We would like to mention that the $\tilde{\chi}_1^\pm - \tilde{\chi}_1^0$ and the $\tilde{\tau}_1 - \tilde{\chi}_1^0$ coannihilation scenarios are very general DM coannihilation scenarios, and their features are well studied in many SUSY models. If neutralino has a large higgsino component with a small μ value the chargino should also have a large higgsino component and their masses can be nearly degenerate. This is the case for the $\tilde{\chi}_1^\pm - \tilde{\chi}_1^0$ coannihilation. When neutralino is bino dominant, $\tilde{\chi}_1^0$ usually has large mass gap with the chargino. In this case it needs to coannihilate with the other NLSP. If there is some kind of unification at high energy scales, squarks are generally heavy since gauge couplings tend to lift their masses when running from high energy scale to low scale. In this case, the lightest scalar sparticle at low energy usually is the lighter stau. Therefore the $\tilde{\tau}_1 - \tilde{\chi}_1^0$ coannihilation is another important and common case to give correct DM relic density. It is very important to study these two coannihilation cases and consider their implications for SUSY search at the LHC.

In the $\tilde{\chi}_1^\pm - \tilde{\chi}_1^0$ coannihilation scenario, we concentrate on the process $pp \rightarrow \tilde{t}_1 \tilde{t}_1^* \rightarrow b\bar{b} \tilde{\chi}_1^+ \tilde{\chi}_1^-$, and put constraints on the parameter space by using the LHC b-jets + \cancel{E}_T results. We find that the ATLAS and CMS searches at $\sqrt{s} = 7$ TeV can exclude a region up to $m_{\tilde{t}_1} \simeq 380$ GeV. The region corresponding to $S/\sqrt{B} > 3$ expected at $\sqrt{s} = 8$ TeV for 20 fb^{-1} almost covers all the space in the $m_{\tilde{t}_1} - m_{\tilde{\chi}_1^\pm}$ plane for $m_{\tilde{\chi}_1^\pm} \lesssim 280$ GeV and $m_{\tilde{t}_1} \lesssim 430$ GeV.

In the $\tilde{\tau}_1 - \tilde{\chi}_1^0$ coannihilation scenario, we focus on the process $pp \rightarrow \tilde{t}_1 \tilde{t}_1^* \rightarrow b\bar{b} \nu_\tau \bar{\nu}_\tau \tilde{\tau}_1^+ \tilde{\tau}_1^-$, which is more difficult than the case in the $\tilde{\chi}_1^\pm - \tilde{\chi}_1^0$ coannihilation scenario, due to the neutrinos from \tilde{t}_1 decay. We find that only a small region up to $m_{\tilde{t}_1} \simeq 220$ GeV is excluded by 7 TeV LHC searches. At $\sqrt{s} = 8$ TeV for 20 fb^{-1} , the expected $S/\sqrt{B} = 3$ limit reaches $m_{\tilde{\tau}_1} \simeq 240$ GeV and $m_{\tilde{t}_1} \simeq 370$ GeV.

Acknowledgments

This work is supported by the Natural Science Foundation of China under the grant NO. 11105157, NO. 11075169, No. 11175251 and NO. 11135009, the 973 project under grant No. 2010CB833000, and the Chinese Academy of Science under Grant No. KJCX2-EW-W01.

-
- [1] G. Bertone, D. Hooper and J. Silk, Phys. Rept. **405**, 279 (2005) [hep-ph/0404175].
 - [2] G. Jungman, M. Kamionkowski and K. Griest, Phys. Rept. **267**, 195 (1996) [hep-ph/9506380].
 - [3] D. Larson *et al.*, Astrophys. J. Suppl. **192**, 16 (2011) [arXiv:1001.4635 [astro-ph.CO]].
 - [4] A. Fowlie, M. Kazana, K. Kowalska, S. Munir, L. Roszkowski, E. M. Sessolo, S. Trojanowski and Y. -L. S. Tsai, Phys. Rev. D **86**, 075010 (2012) [arXiv:1206.0264 [hep-ph]].
 - [5] K. Griest and D. Seckel, Phys. Rev. D **43**, 3191 (1991).
 - [6] J. Edsjo and P. Gondolo, Phys. Rev. D **56**, 1879 (1997) [hep-ph/9704361].
 - [7] J. R. Ellis, T. Falk and K. A. Olive, Phys. Lett. B **444**, 367 (1998) [hep-ph/9810360].
 - [8] S. Profumo and C. E. Yaguna, Phys. Rev. D **69**, 115009 (2004) [hep-ph/0402208].
 - [9] C. Boehm, A. Djouadi and M. Drees, Phys. Rev. D **62**, 035012 (2000) [hep-ph/9911496].
 - [10] S. Profumo, Phys. Rev. D **68**, 015006 (2003) [hep-ph/0304071].
 - [11] M. Adeel Ajaib, T. Li, Q. Shafi, K. Wang, JHEP **1101**, 028 (2011) [arXiv:1011.5518 [hep-ph]].
 - [12] N. Chen, D. Feldman, Z. Liu, P. Nath and G. Peim, Phys. Rev. D **83**, 035005 (2011) [arXiv:1011.1246 [hep-ph]].
 - [13] M. Adeel Ajaib, T. Li and Q. Shafi, Phys. Lett. B **701**, 255 (2011) [arXiv:1104.0251 [hep-ph]]; Phys. Lett. **B705**, 87-92 (2011) [arXiv:1107.2573 [hep-ph]]; Phys. Rev. D **85**, 055021 (2012) [arXiv:1111.4467 [hep-ph]]; B. He, T. Li and Q. Shafi, JHEP **1205**, 148 (2012) [arXiv:1112.4461 [hep-ph]].
 - [14] X. -J. Bi, Q. -S. Yan and P. -F. Yin, Phys. Rev. D **85**, 035005 (2012) [arXiv:1111.2250 [hep-ph]].
 - [15] M. Drees, M. Hanussek and J. S. Kim, Phys. Rev. D **86**, 035024 (2012) [arXiv:1201.5714 [hep-ph]].

- [16] S. Chatrchyan *et al.* [CMS Collaboration], arXiv:1207.1898 [hep-ex].
- [17] G. Aad *et al.* [ATLAS Collaboration], arXiv:1208.0949 [hep-ex].
- [18] M. Carena, A. Freitas and C. E. M. Wagner, JHEP **0810**, 109 (2008) [arXiv:0808.2298 [hep-ph]].
- [19] P. J. Fox, R. Harnik, J. Kopp and Y. Tsai, Phys. Rev. D **85**, 056011 (2012) [arXiv:1109.4398 [hep-ph]].
- [20] R. Kitano and Y. Nomura, Phys. Rev. D **73**, 095004 (2006) [hep-ph/0602096]; M. Papucci, J. T. Ruderman and A. Weiler, arXiv:1110.6926 [hep-ph].
- [21] M. Carena, G. Nardini, M. Quiros, C. E. M. Wagner, JHEP **0810**, 062 (2008) [arXiv:0806.4297 [hep-ph]]; Nucl. Phys. **B812**, 243-263 (2009) [arXiv:0809.3760 [hep-ph]].
- [22] G. Aad *et al.* [ATLAS Collaboration], arXiv:1208.1447 [hep-ex].
- [23] G. Aad *et al.* [ATLAS Collaboration], arXiv:1208.2590 [hep-ex].
- [24] A. Choudhury and A. Datta, JHEP **1206**, 006 (2012) [arXiv:1203.4106 [hep-ph]].
- [25] H. Baer, V. Barger, P. Huang and X. Tata, JHEP **1205**, 109 (2012) [arXiv:1203.5539 [hep-ph]].
- [26] X. -J. Bi, Q. -S. Yan and P. -F. Yin, arXiv:1209.2703 [hep-ph].
- [27] S. Profumo and C. E. Yaguna, Phys. Rev. D **70**, 095004 (2004) [hep-ph/0407036].
- [28] J. Alwall, M. Herquet, F. Maltoni, O. Mattelaer and T. Stelzer, JHEP **1106**, 128 (2011) [arXiv:1106.0522 [hep-ph]].
- [29] T. Sjostrand, S. Mrenna and P. Z. Skands, JHEP **0605**, 026 (2006) [arXiv:hep-ph/0603175].
- [30] PGS-4, J. Conway *et al.*, <http://www.physics.ucdavis.edu/~conway/research/software/pgs/pgs4-general.htm>.
- [31] W. Beenakker, R. Hopker and M. Spira, arXiv:hep-ph/9611232.
- [32] J. Campbell, R. Ellis and C. Williams, <http://mcfm.fnal.gov>.
- [33] G. Aad *et al.* [The ATLAS Collaboration], arXiv:1210.4491 [hep-ex].
- [34] S. Chatrchyan *et al.* [CMS Collaboration], JHEP **1209**, 094 (2012) [arXiv:1206.5663 [hep-ex]].
- [35] CDF collaboration, CDF-Note 9834, http://www-cdf.fnal.gov/physics/exotic/r2a/20090709.stop_charm/.
- [36] G. Aad *et al.* [ATLAS Collaboration], Phys. Rev. Lett. **108**, 181802 (2012) [arXiv:1112.3832 [hep-ex]].
- [37] The ATLAS Collaboration, ATLAS-CONF-2012-106 (2012).
- [38] S. Chatrchyan *et al.* [CMS Collaboration], Phys. Rev. D **86**, 072010 (2012) [arXiv:1208.4859 [hep-ex]].